J Mater Sci: Mater Med (2012) 23:2831–2837
DOI 10.1007/s10856-012-4743-y

Microwave assisted synthesis of amorphous magnesium phosphate nanospheres

Huan Zhou · Timothy J. F. Luchini · Sarit B. Bhaduri

Received: 25 May 2012 / Accepted: 2 August 2012 / Published online: 14 August 2012

Abstract Magnesium phosphate (MgP) materials have been investigated in recent years for tissue engineering applications, attributed to their biocompatibility and biodegradability. This paper describes a novel microwave assisted approach to produce amorphous magnesium phosphate (AMP) in a nanospherical form from an aqueous solution containing Mg^{2+} and HPO_4^{2-}/PO_4^{3-}. Some synthesis parameters such as pH, Mg/P ratio, solution composition were studied and the mechanism of AMP precursors was also demonstrated. The as-produced AMP nanospheres were characterized and tested in vitro. The results proved these AMP nanospheres can self-assemble into mature MgP materials and support cell proliferation. It is expected such AMP has potential in biomedical applications.

1 Introduction

Calcium containing biomaterials, such as calcium phosphate (CaP), calcium sulfate ($CaSO_4$) and calcium silicate (CS) are traditionally researched inorganic biomaterials used for bone regeneration [1–3]. Being in the same period of the periodic table with calcium makes magnesium one of the main substitutes for calcium in biological apatite. It is known magnesium can influence the bone mineral metabolism, formation and crystallization processes [4, 5]. Consequently, doping calcium containing biomaterials with magnesium has recently become an active topic in biomaterial research. It was reported that CaP doped with magnesium can be stabilized, significantly enhancing osteoblast attachment and growth as compared to pure CaP [6, 7]. Similarly, a calcium magnesium silicate bioceramic (Akermanite) promoted more osteogenesis, biodegradation, and bone formation once implanted in rabbit test subjects than β-tricalcium phosphate (β-TCP) [8]. Additionally, bone cement doped with magnesium showed controllable degradability and great mechanical and biological performance as compared to CaP bone cement (CPC) [9].

Instead of doping calcium based biomaterials with magnesium, there is a current trend directly using magnesium based materials as a potential alternative for orthopedic applications. One such area of research uses magnesium alloys as implant materials, which are lightweight, degradable, load bearing, biocompatible, and possibly biologically active [10]. The deposition of a magnesium coating on metallic implants to induce the formation of a uniform bioactive coating has been reported [11]. Magnesium phosphate (MgP) is another area of recent focus. MgP is biocompatible and exhibits a faster biodegradation rate compared to CaP [12]. Reported MgP bone cements (MPC) show all the functions necessary for potential bone cement applications including injectability, degradability, biocompatibility, high strength and suitable setting time for clinical applications [13–16]. Additionally, MgP nanoparticles have been applied to gene delivery and in vitro DNA transfection in HeLa cells demonstrating that MgP nanoparticles show almost 100 % transfection efficiency [17].

The formation of MgP is based on the ionic interaction between Mg^{2+} and PO_4^{3-} in aqueous medium. Generally, in synthesis processes, different MgP materials such as $MgHPO_4{\cdot}3H_2O$, $Mg_3PO_4{\cdot}5H_2O$, $Mg_3PO_4{\cdot}8H_2O$,

H. Zhou (✉) · T. J. F. Luchini · S. B. Bhaduri
Department of Mechanical, Industrial and Manufacturing Engineering, University of Toledo, Toledo, OH, USA
e-mail: Huan.Zhou@rockets.utoledo.edu

S. B. Bhaduri
Dentistry, Department of Surgery, University of Toledo, Toledo, OH, USA

$Mg_3PO_4{\cdot}22H2O$, and $Mg_2PO_4OH{\cdot}4H_2O$ can be precipitated under conditions such as Mg/P ratio, temperature, and pH [18, 19]. Alternatively, NH_4^+ or Ca^{2+} from aqueous medium can substitute into the MgP lattice, which develops into a good bone substitute biomaterial [12–14].

A survey of literature shows that kinetic study of MgP nucleation and precipitation in physicological conditions is rare. Previously reported research only focuses on the final precipitated MgP minerals by controlling reaction conditions such as temperature and ionic composition [18, 19]. In contrast, CaP growth from precursors to mature crystals has been systematically studied and illustrated [20–22]. The main problem in studying the kinetics of MgP formation is to prepare MgP precursors on the nano scale and evaluate their transformation under certain environments. Unfortunately, the synthesis of MgP nano precursors is more difficult than CaP precursors, limited by the high instability of MgP in aqueous medium. In our previous research source, we reported a microwave (MW) assisted method to produce amorphous CaP nano precursors [23]. In the report it is observed that Mg^{2+} can be incorporated into the CaP lattice and the weight ratio of Mg increases with its concentration in aqueous medium. This MW assisted method can be a potential strategy to prepare MgP nano precursors.

In this study two concepts are evaluated: (1) potential preparation of Amorphous Magnesium Phosphate (AMP) precursors on the nano scale using MW irradiation, (2) MgP growth using prepared AMP precursors in a physiological environment of simulated body fluid (SBF). In addition, to ensure the synthesized particles from MW assisted pathways are biocompatible materials suitable for potential bone tissue engineering applications, selected MgP precursors are used for bone osteoblast growth.

2 Materials and methods

2.1 Preparation and characterization of AMP precursors

All reagent grade chemicals were purchased from Fisher Scientific (NJ, USA) and used without further purification.

The reaction solutions were prepared by mixing $MgCl_26H_2O$, KH_2PO_4 and $NaHCO_3$ in 1 L DI water in 3 L capacity beaker. The reactants were dissolved in DI water one by one, and added based on the order listed in Table 1. In addition, 1 M NaOH and 1 M HCl solutions were prepared for adjusting pH of the prepared solutions to the values as shown in Table 1. The solutions had two different magnesium concentrations: (1) physiological condition in human plasma (1.5 mM Mg^{2+}) denoted with L; (2) 10× more concentrated than physiological condition (15 mM Mg^{2+}) denoted with H. Furthermore, three different Mg/P molar ratios were applied (3:2, 2:3, 1:1), though Mg/P molar ratio in human plasma/serum ranged from 3:2 to 2:3 [24, 25]. The one low concentration sample tested is denoted L1 and the six high concentration samples are denoted H1–H6 for simplicity. The addition of $NaHCO_3$ mimics human plasma and works as a pH buffer. The pH value of each solution was measured using a pH meter (Mettler Toledo, OH, USA).

Table 1 Compositions of tested solutions

Solution	$NaHCO_3$	$MgCl_2{\cdot}6H_2O$	KH_2PO_4	pH	Mg/P
L1	0.227	0.2078	0.1361	6.8	1:1
H1	2.27	2.078	1.361	6.8	1:1
H2	2.27	3.116	1.361	6.8	3:2
H3	2.27	1.385	1.361	6.8	2:3
H4	2.27	2.078	1.361	5	1:1
H5	2.27	2.078	1.361	8	1:1
H6	2.27	2.078	1.361	9	1:1

One low concentration sample denoted L1 is tested and six high concentration samples are tested denoted H1–H6 for simplicity

Sample beakers of 150 mL with 100 mL prepared solution were then placed onto 10 × 10 × 1 cm alumina insulating fiberboards and covered with an upside down 250 mL-capacity glass beaker. To proceed with the MW assisted process, the sample assembles were placed into a household MW oven (Emerson, max. power 100 W, 2450 MHZ, NJ, USA) for 5 min. At the end of MW heating, the samples were moved to a cold water bath to cool down. Finally, the precipitates were collected after centrifuging at 3,000×g rpm for 5 min followed by rinsing using DI water to remove residual salts. All precipitates were completely dried in a 37 °C oven overnight.

2.2 Evaluating the activity of AMP nano precursors in SBF

SBF was prepared following the recipe reported by before [26, 27], with an ionic composition closely mimicking

Table 2 Composition of 1 L test SBF

Order	Reagent	SBF
1	NaCl	6.5456 g
2	$NaHCO_3$	2.2682 g
3	KCl	0.3727 g
4	Na_2HPO_4	0.1419 g
5	$MgCl_2{\cdot}6H_2O$	0.3045 g
6	1 M HCL	10 mL
7	$CaCl_2{\cdot}2H_2O$	0.3881 g
8	Na_2SO_4	0.072 g
9	Tris-Base	6.063 g
10	1 M HCl	33.3 mL

human body plasma. The composition is shown in Table 2. The reagents were dissolved in solution one by one in the order listed in Table 2 and stored at 5 °C when not in use. Each 0.5 g dried powder was bottled in 40 mL of SBF separately. All samples were incubated in a 37 °C environment for 7 days with SBF replenished every 48 h. Finally, powders were collected via centrifuge and dried in an oven for further characterization.

2.3 Characterization

All powders were characterized by X-ray diffraction (XRD, Ultima III, Rigaku)) with monochromated Cu Kα radiation operated at a voltage of 40 kV and a current set at 44 mA. The morphological features of precipitates and incubated powders were visualized using a scanning electron microscope (SEM, S4800, Hitachi). Energy dispersive X-ray spectroscopy (EDS) in an SEM was used to analyze the powders elemental composition and molar ratio. The inner structure of AMP nanospheres was investigated via transmission electron microscopy (TEM, HD-2300, Hitachi) with a 200 kV voltage.

2.4 Preliminary cell culture on AMP

Mouse 7F2 osteoblast cells (CRL-12557, American Type Culture Collection) were used for the cell culture on powders from H1. Osteoblast cells were first grown at 37 °C and 5 % CO_2 in alpha minimum essential medium (α-MEM, Thermo Scientific HyClone), augmented by 10 % fetal bovine serum (FBS, Thermo Scientific HyClone). MgP pellets were prepared by pressing MgP powders in a die. These pressed pellets were stable in an aqueous environment. Harvested osteoblasts were seeded onto sterilized MgP pellets. Osteoblast morphology on samples after 3 days was examined using SEM. Prior to SEM, samples underwent a fixation procedure with glutaraldehyde, graded dehydration with ethanol, critical point drying procedure and sputter coating [27, 28].

3 Results

MgP solution at physiological ionic concentration (1× denoted L) does not form precipitates after 5 min of MW irradiation. Alternatively, precipitates are observed from more concentrated MgP solutions (10× denoted H). However, solutions with a pH of 5 cannot form precipitates after MW treatment. While a solution with a pH of 9 can spontaneously start precipitating at room temperature without any further MW irradiation. All the results are shown in Table 3.

Table 3 Results of MgP precipitation from different solutions

Solution	Precipitation	Stability at room temperature	Mg/P
L1	No	Stable	N/A
H1	Yes	Stable	1.285 ± 0.24
H2	Yes	Stable	1.23 ± 0.07
H3	Yes	Stable	0.973 ± 0.29
H4	No	Stable	N/A
H5	Yes	Stable	1.292 ± 0.11
H6	Yes	Precipitation	1.308 ± 0.21

One low concentration sample denoted L1 is tested and six high concentration samples are tested denoted H1–H6 for simplicity

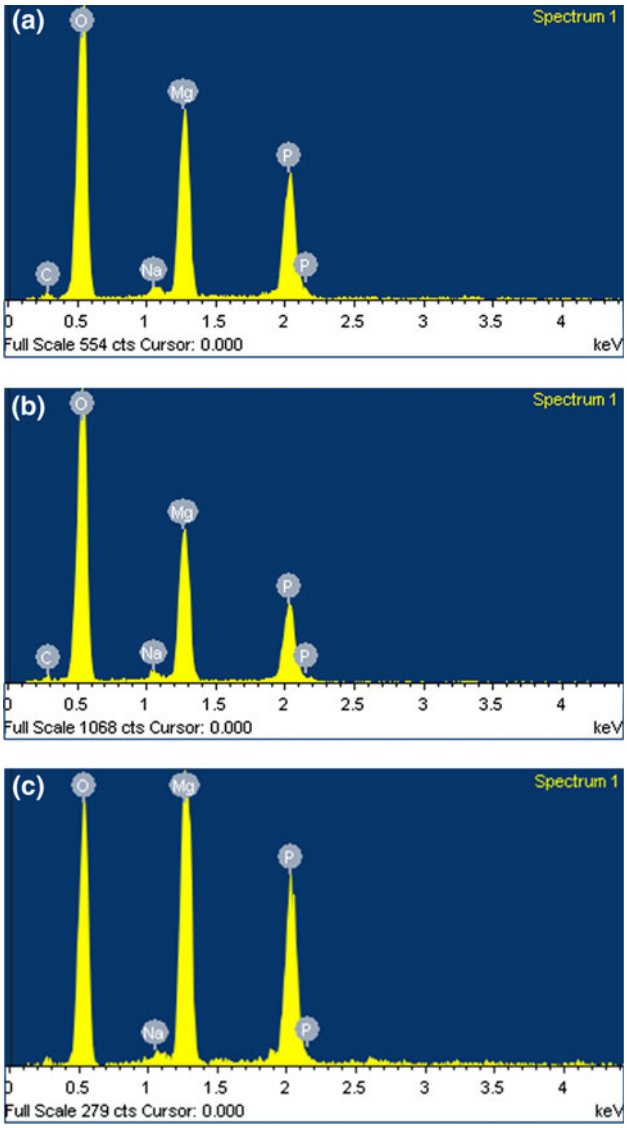

Fig. 1 EDS results of MgP precipitates from different solution **a** H1, **b** H5, and **c** H6

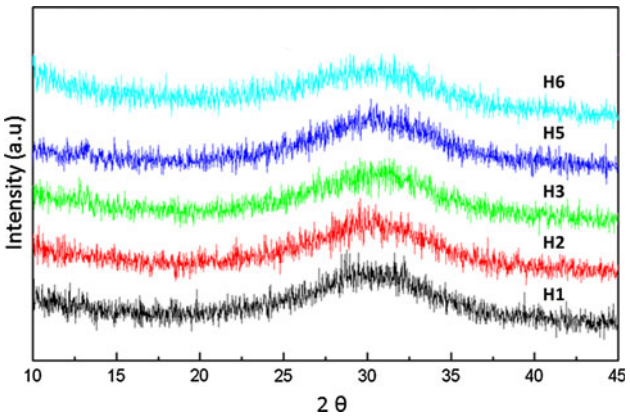

Fig. 2 XRD results of MgP precipitates from different solutions

EDS results indicate the precipitates from MgP solutions are mainly composed of Mg^{2+} and PO_4^{3-} (Fig. 1). Ionic concentration, Mg/P molar ratio and pH showed impacts on the Mg/P molar ratio of resulting precipitates (Table 3).

XRD analysis of the precipitates (Fig. 2) reveals that the formed materials are amorphous, resulting the formation of a broad peak with its maximum intensity at 31 degree, confirming the synthesized MgP precipitates are AMP.

The SEM results of precipitates are listed in Fig. 3. AMP nanospheres are successfully synthesized via MW irradiation from H1, H2, H3 and H5. Different Mg/P molar ratios have no significant impacts on the morphology of formed nanospheres. A high pH results in more uniform nanosphere diameters as compared to lower pH values. The nanospheres from H3 show the minimum diameter nanospheres based on the measuring the diameters of spheres in SEM images. On the other hand, precipitates (H6) forming by spontaneous precipitation at room temperature due to a higher pH of 9 are in the shape of plates.

The TEM data in Fig. 4a shows the densely composed structure of the prepared AMP nanospheres. In Fig. 4b, the bonding between fused AMP nanospheres is shown.

After 7 days of SBF incubation, there are significant crystal and structure changes to precipitated AMP materials. XRD analysis (Fig. 5) shows the transition from AMP materials to mature Bobierrite ($Mg_3PO_4{\cdot}8H_2O$) [16]. SEM results (Fig. 6) indicate AMP materials assemble into crystals with a layered structure of ellipses and cylinders. Precipitates from H6 convert into a plate structure composed of several crystals with sub-layered structures again formed from ellipses and cylinders. Observations of Ca^{2+} ions are seen incorporating into the MgP lattice structure from EDS (data not included) and CaP apatites are deposited on MgP precipitate surfaces. Consequently, both AMP nanospheres and plates can be converted into mature $Mg_3PO_4{\cdot}8H_2O$ after 7 days of SBF incubation.

Cell attachment on an AMP pellet is shown in Fig. 7a, osteoblasts can be seen proliferating on the AMP sample surface. This confirms that AMP nanospheres synthesized from MW irradiation are biocompatible. In addition, the features of AMP pellets are also characterized. After 3 days of culture medium incubation the AMP nanospheres are assembled into large particles (Fig. 7b), similar to the phenomenon in seen after SBF soaking. The surface of MgP after incubation exhibits a porous structure in some areas (Fig. 7c) possibly from MgP dissolution.

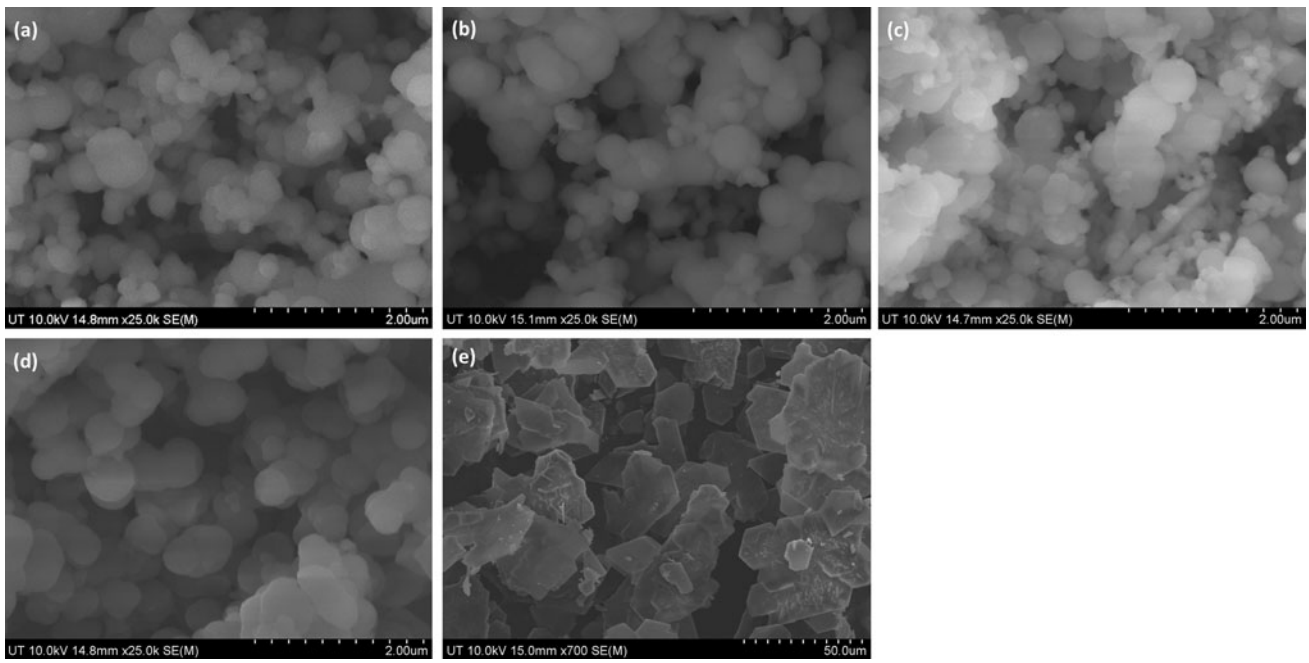

Fig. 3 SEM images of MgP precipitates from solutions **a** H1, **b** H2, **c** H3, **d** H5, and **e** H6

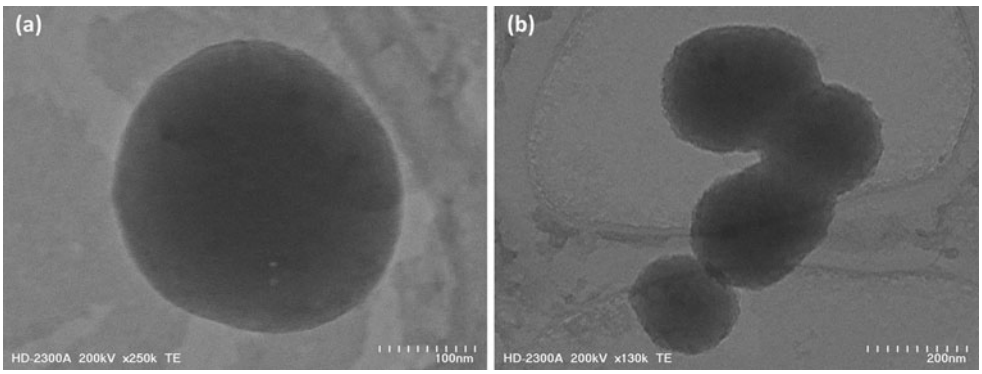

Fig. 4 TEM images of MgP nanospheres. **a** Single nanosphere. **b** Fused nanospheres

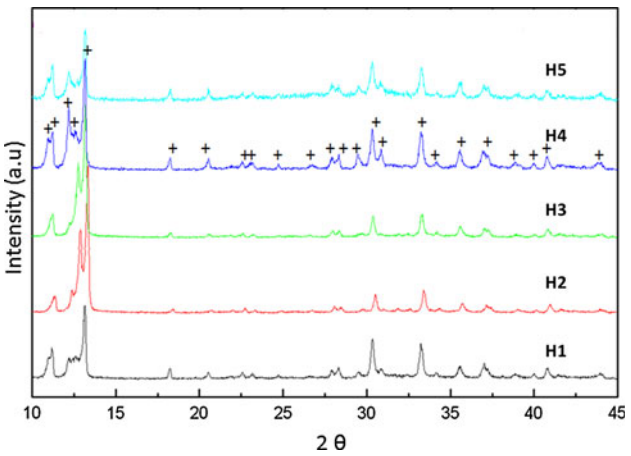

Fig. 5 XRD of MgP precipitates after 7 d SBF incubation, '+' represents $Mg_3PO_4{\cdot}8H_2O$

4 Discussion

AMP in a nanospherical shape is successfully prepared using MW irradiation based on the results of XRD, SEM and EDS. It is a simple, rapid, controllable and repeatable reaction system for preparing MgP precursors. It is the first time reporting the synthesis of AMP precursors. Additionally, prepared AMP precursors show the ability to be converted into mature MgP materials at physiological conditions through experimentation.

Formation of amorphous CaP nanospherical precursors from concentrated SBF by MW irradiation has been illustrated by Zhou et al. [23]. In the MW irradiation system, nanospherical CaP is the most energy efficient structure because the conversion from precursors to mature CaP is inhibited by energy barriers. In this new MgP precipitation application, the mechanism also partially works, attributed to the similar chemical properties of Mg^{2+} to Ca^{2+}. In the concentrated MgP solution, AMP is the first phase to precipitate compared to other MgP materials such as $MgHPO_4{\cdot}3H_2O$, $Mg_3PO_4{\cdot}5H_2O$, $Mg_3PO_4{\cdot}8H_2O$, and $Mg_3PO_4{\cdot}22H_2O$. The presence of MgP precursors in solution and the high reaction temperature caused by MW irradiation can trigger an irreversible MgP precipitation phenomenon similar to the reported amorphous CaP precipitation [23]. However, the conversion from AMP to other MgP materials is supposed to be a process requiring extra energy. In contrast, the formation of AMP has no such energy requirement under MW irradiation, thus more and more AMP precursors are precipitated from the solution with high concentrations of Mg^{2+} and PO_4^{3-}/HPO_4^{2-}. In previous amorphous CaP precipitation experiments source, it is observed that the obtained CaP precursors are very active and can only be stabilized by incorporating Mg^{2+} to the lattice structure [23]. Nevertheless, the prepared MgP nanospherical precursors preserved their shape in comparison to CaP. This difference can be attributed to the difference in crystal growth kinetics between CaP and MgP. Growth of CaP is a process absorbing free Ca^{2+} and PO_4^{3-}/HPO_4^{2-} ions to form CaP crystals and hydrated ions from the core of CaP precursors [20]. In contrast, MgP growth is a process assembling formed AMP precursors together, Mg^{2+} and $PO4^{3-}/HPO_4^{2-}$ in amorphous structure fused to each other (Fig. 4b). Such assembly phenomenon also requires extra energy, which is consequently inhibited in MW irradiation. However, during the period of cooling down, these nanospheres start fusing to each other.

In addition, both CaP and MgP precipitation under MW irradiation can be influenced by starting pH, ionic concentration, solution composition [23], similar to the conventional precipitation in aqueous medium [19, 29]. At a low pH 5, no precipitation of MgP can occur, while a high pH is a factor to accelerate crystal growth, as well as high ionic concentration. With the continuing precipitation, the ionic concentration continues decreasing, thus the formation of smaller MgP nanospheres results. The difference in the minimum nanosphere diameter observed in Fig. 3a, b, c, d can therefore be attributed to a combined effect of

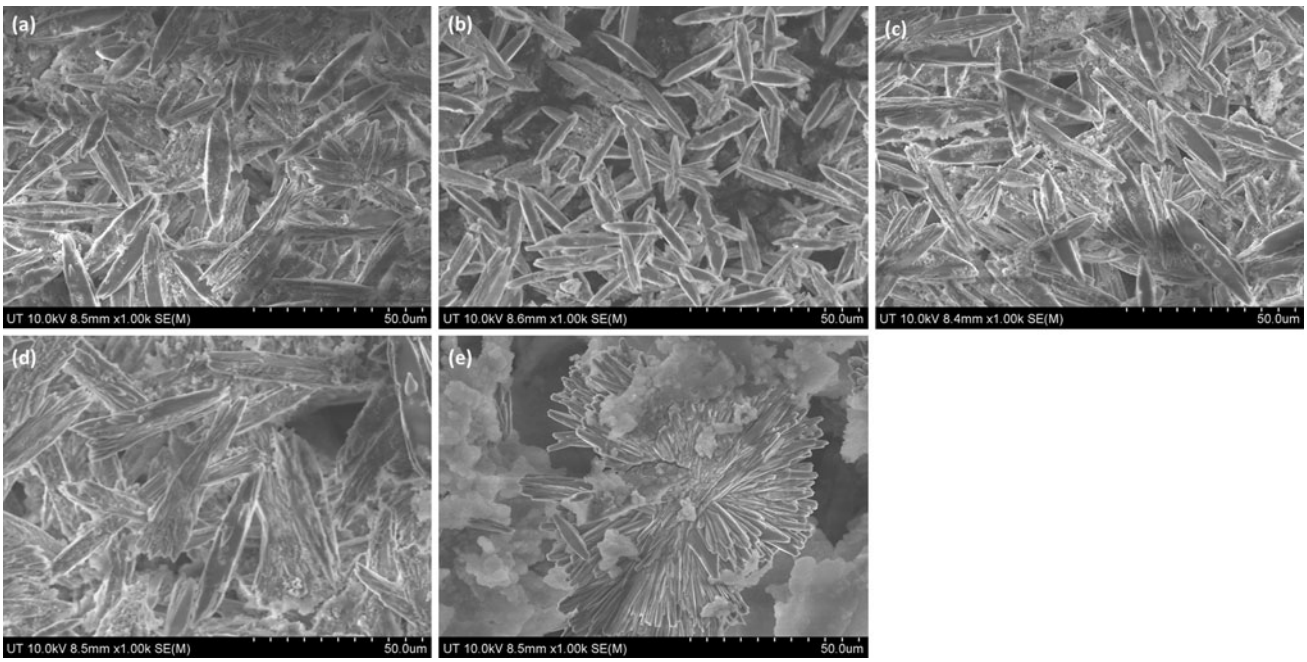

Fig. 6 SEM images of MgP precipitates after 7 d SBF incubation **a** H1, **b** H2, **c** H3, **d** H5, and **e** H6

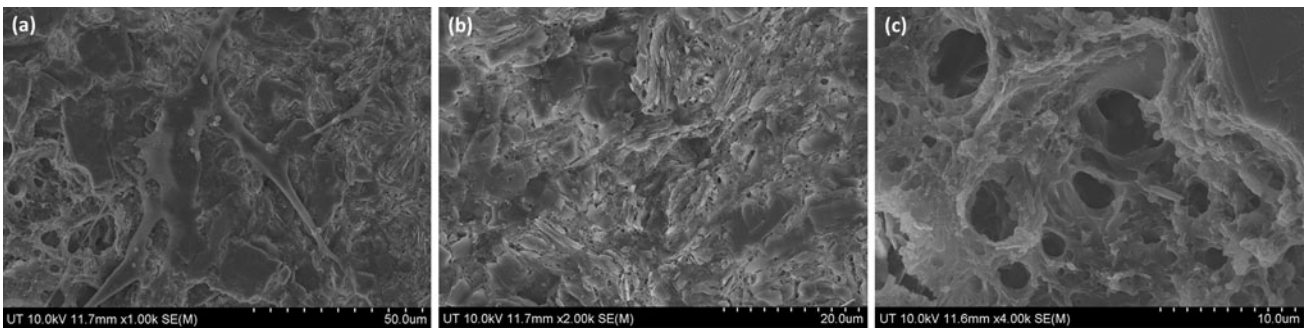

Fig. 7 3d cell culture results. **a** Cells morphology on MgP pellet. **b** MgP surface feature. **c** MgP surface pores

ionic concentration decrease during reaction, pH difference and varied Mg/P molar ratio. H3 formed the nanospheres with the minimum diameter because it has the lowest pH and ionic concentration.

After 7 days of SBF incubation, the prepared MgP precursors show a similar structure transition to amorphous MgP plates (H6), confirming these MgP precursors can be a potential tool for MgP crystal growth analysis. However, the mechanism of such structure transition is not clear, possibly being related to hydrolysis and crystallization. An additional kinetic study using environmental SEM is necessary in future.

Evaluations via SEM show that AMP nanospheres are potential candidates for orthopedic applications because of cell proliferation on synthesized AMP surfaces. The fusion of AMP nanospheres to MgP particles provides information on the growth kinetics of MgP. Potential applications are the study of the MgP cement setting and kidney stone formation from MgP in the presence of urea. However, a systematic in vitro study of AMP nanospheres is necessary in the future to evaluate the biocompatibility of AMP.

One important difference of MgP behavior in tissue engineering as compared to CaP is its biodegradability, CaP due to the presence of Mg^{2+} on the material surface, thus making the deposited CaP apatite highly amorphous. It is well known for CaP materials, their dissolution rate is correlated to their crystallinity [30]. For most biodegradable materials, the stable apatite deposition onto their surface can significantly delay their dissolution. One classic example is Brushite, which exhibits high dissolution at its initial stage, but once apatite formed on its surface its dissolution is completely stopped [31]. Such phenomenon will not occur on MgP surface. This fact may be taken advantage of in bone tissue engineering.

5 Conclusion

In conclusion, this study shows a novel MW assisted process to synthesize AMP precursors in nanospherical forms from a solution containing Mg^{2+} and HPO_4^{2-}/PO_4^{3-}. The mechanism behind this approach and related experimental factors such as pH, Mg/P ratio, solution ionic concentration have been studied. The as-synthesized AMP precursors show the ability to convert into other MgP materials, thus providing a tool for studying the MgP growth kinetic in the body or in different environments. However, this work is just a preliminary study of AMP, more systematic studies are necessary in future to evaluate their biocompatibility and biodegradablity and prove their potentials in tissue engineering applications.

References

1. Dorozhkin SV, Epple M. Biological and medical significance of calcium phosphates. Angew Chem Int Ed. 2002;41:3130–46.
2. Zhao W, Wang J, Zhai W, Wang Z, Chang J. The self-setting properties and in vitro bioactivity of tricalcium silicate. Biomaterials. 2005;26:6113–21.
3. Thomas MV, Puleo DA. Calcium sulfate: properties and clinical applications. J Biomed Mater Res B Appl Biomater. 2009;88:597–610.
4. Rude RK, Gruber HE, Wei LY, Frausto A, Mills BG. Magnesium deficiency: effect on bone and mineral metabolism in the mouse. Calcif Tissue Int. 2003;72:32–41.
5. Salimi MH, Heughebaert JC, Nancollas GH. Crystal growth of calcium phosphates in the presence of magnesium ions. Langmuir. 1985;1:119–22.
6. Xue W, Dahlquist K, Banerjee A, Bandyopadhyay A, Bose S. Synthesis and characterization of tricalcium phosphate with Zn and Mg based dopants. J Mater Sci Mater Med. 2008;19:2669–77.
7. Paul W, Sharma CP. Effect of calcium, zinc and magnesium on the attachment and spreading of osteoblast like cells onto ceramic matrices. J Mater Sci Mater Med. 2007;18:699–703.
8. Huang Y, Jin X, Zhang X, Sun H, Tu J, Tang T, et al. In vitro and in vivo evaluation of akermanite bioceramics for bone regeneration. Biomaterials. 2009;30:5041–8.
9. Lu J, Wei J, Yan Y, Li H, Jia J, Wei S, et al. Preparation and preliminary cytocompatibility of magnesium doped apatite cement with degradability for bone regeneration. J Mater Sci Mater Med. 2011;22:607–15.
10. Staiger MP, Pietak AM, Huadmai J, Dias G. Magnesium and its alloys as orthopedic biomaterials: a review. Biomaterials. 2006;27:1728–34.
11. Ibasco S, Tamimi F, Meszaros R, Nihouannen DL, Vengallatore S, Harvey E, et al. Magnesium-sputtered titanium for the formation of bioactive coatings. Acta Biomater. 2009;5:2338–47.
12. Klammert U, Ignatius A, Wolfram U, Reuther T, Gbureck U. In vivo degradation of low temperature calcium and magnesium phosphate ceramics in a heterotopic model. Acta Biomater. 2011;7:3469–75.
13. Mestres G, Ginebra MP. Novel magnesium phosphate cements with high early strength and antibacterial properties. Acta Biomater. 2011;7:1853–61.
14. Jia J, Zhou H, Wei J, Jiang X, Hua H, Chen F, et al. Development of magnesium calcium phosphate biocement for bone regeneration. J R Soc Interface. 2010;7:1171–80.
15. Klammert U, Vorndran E, Reuther T, Muller FA, Zorn K, Gbureck U. Low temperature fabrication of magnesium phosphate cement scaffolds by 3D powder printing. J Mater Sci Mater Med. 2010;21:2947–53.
16. Aramendia MG, Borau V, Jimenez C, Marinas JM, Romero F. J. Synthesis and characterization of magnesium phosphates and their catalytic properties in the conversion of 2-hexanol. J Colloid Interface Sci. 1999;217:288–98.
17. Bhakta G, Mitra S, Maitra A. DNA encapsulated magnesium and manganous phosphate nanoparticles: potential non-viral vectors for gene delivery. Biomaterials. 2005;26:2157–63.
18. Kurtulus G, Tas AC. Transformations of neat and heated struvite (MgNH4PO4·6H2O). Mater Lett. 2011;65:2883–6.
19. Tamimi F, Le Nihouannen D, Bassett DC, Ibasco S, Gbureck U, Knowles J, et al. Biocompatibility of magnesium phosphate minerals and their stability under physiological conditions. Acta Biomater. 2011;7:2678–85.
20. Tao J, Pan H, Wang J, Wu J, Wang B, Xu X, et al. Evaluation of amorphous calcium phosphate to hydroxyapatite probed by gold nanoparticles. J Phys Chem C. 2008;112:14929–33.
21. Francis MD, Webb NC. Hydroxyapatite formation from a hydrated calcium monoydrogen phosphate precursor. Calcif Tiss Res. 1971;6:335–42.
22. Posner AS, Betts F. Synthetic amorphous calcium phosphate and its relation to bone mineral structure. Acc Chem Res. 1975;8:273–81.
23. Zhou H, Bhaduri S. Novel microwave synthesis of amorphous calcium phosphate nanospheres. J Biomed Mater Res B Appl Biomater. 2012;100:1142–50.
24. Oyane A, Kim H-M, Furuya T, Kokubo T, Miyazaki T, Nakamura T. Preparation and assessment of revised simulated body fluids. J Biomed Mater Res A. 2003;65:188–95.
25. Weisinger JR, Bellorín-Font E. Magnesium and phosphorus. Lancet. 1998;352:391–6.
26. Jalota S, Bhaduri SB, Tas AC. Effect of carbonate content and buffer type on calcium phosphate formation in SBF solutions. J Mater Sci Mater Med. 2006;17:697–707.
27. Zhou H, Lawrence JG, Touny AH, Bhaduri SB. Biomimetic coating of bisphosphonate incorporated CDHA on Ti6Al4V. J Mater Sci Mater Med. 2012;23:365–74.
28. Zhou H, Touny A, Bhaduri S. Fabrication of novel PLA/CDHA bionanocomposite fibers for tissue engineering applications via electrospinning. J Mater Sci Mater Med. 2011;22:1183–93.
29. Tas AC, Bhaduri SB. Rapid coating of Ti6Al4V at room temperature with a calcium phosphate solution similar to 10× simulated body fluid. J Mater Res. 2004;19:2742–9.
30. Combes C, Rey C. Amorphous calcium phosphates: synthesis, properties and uses in biomaterials. Acta Biomater. 2010;6:3362–78.
31. Constantz BR, Barr BM, Ison IC, Fulmer MT, Baker J, McKinney L, et al. Histological, chemical, and crystallographic analysis of four calcium phosphate cements in different rabbit osseous sites. J Biomed Mater Res. 1998;43:451–61.